Thermorheological Consequences of Crystalline-Phase Crosslinking in Polyamide Fibers

SHALINI THADANI, HASKELL W. BECKHAM, PRASHANT DESAI, A. S. ABHIRAMAN

School of Textile and Fiber Engineering, Georgia Institute of Technology, Atlanta, Georgia 30332-0295

Received 4 October 1996; accepted 2 January 1997

ABSTRACT: Wet-spun fibers of a diacetylene-containing aliphatic polyamide (PADA 6,22) were exposed to controlled dosages of electron-beam radiation to selectively crosslink the crystalline regions via a topochemical diacetylene to polydiacetylene conversion. For aligned polymer chains in an oriented fiber, the polydiacetylene crosslinks are created perpendicular to the fiber direction; interference microscopy revealed that the refractive index increased in this direction. Dynamic mechanical spectroscopy and torsional modulus measurements showed that the noncrystalline phase remains essentially unaffected by electron-beam irradiation up to 60 Mrad. Thermal stress analysis demonstrated that higher shrinkage stresses are retained by the irradiated fibers at temperatures approaching the effective thermomechanical melting temperature of the nonirradiated fiber (200°C); thermal deformation analysis also revealed that much lower extensions are exhibited by the crystalline-phase crosslinked fibers at these temperatures. The results suggest that crystalline-phase crosslinking of functionally modified semicrystalline polymers constitutes a mechanism for enhancing structural integrity at elevated temperatures without reducing amorphous-phase flexibility. © 1997 John Wiley & Sons, Inc. J Appl Polym Sci **65:** 2613–2622, 1997

Key words: polyamide; diacetylene; fiber; crystalline-phase crosslinking

INTRODUCTION

The structural integrity of an uncrosslinked semicrystalline polymer is lost when it is subjected to temperatures near the melting temperatures of the crystalline domains. Crosslinking in the noncrystalline domains (e.g., by exposure to various forms of radiation) is one way of reducing the fluidlike deformation of the polymer. However, such crosslinking causes loss of flexibility and also changes the diffusional characteristics of the polymer. Furthermore, amorphous-phase crosslinking does not help substantially in achieving dimensional stability at near-melting temperatures. By reinforcing the crystalline structure, the useful properties of the polymer could be retained at temperatures that approach, or even exceed, its inherent melting temperature.

Various methods have been used to modify the cohesiveness of ordered domains in semicrystalline polymers. For example, the hard domains of thermoplastic elastomers have been chemically crosslinked with such agents as peroxides and trifunctional chain extenders.[1] These methods, however, require adverse disruption of the hard-domain packing and organization, which often results in reduction in ultimate tensile strength of the material. Solid-state crosslinking reactions occurring within ordered domains have been used which do not destroy the ordered chain packing. One such reaction is the topochemical polymerization of diacetylenes incorporated along a linear polymer backbone.[2] This occurs in the ordered phase as a regular 1,4 addition polymerization.[3]

Correspondence to: H. W. Beckham.

Contract grant sponsor: Polymer Program Associates of Georgia Tech.

Journal of Applied Polymer Science, Vol. 65, 2613–2622 (1997)

 CCC 0021-8995/97/132613-10

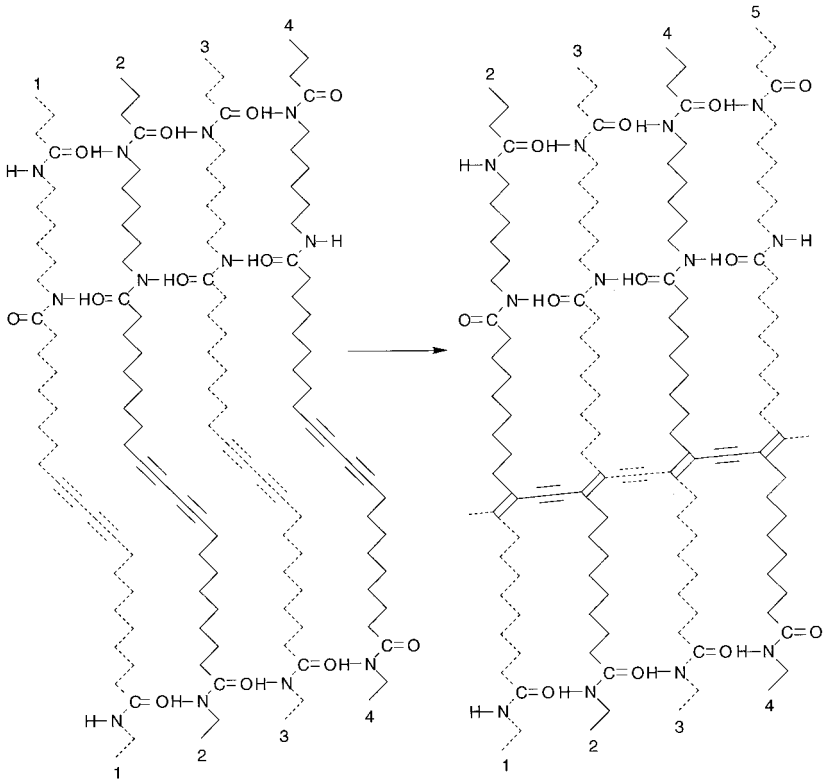

Figure 1 Schematic of PADA 6,22 ordered array before and after cross-polymerization. Consecutive polyamide backbones are represented by dashed and solid lines to aid visualization. Numbers identify the polyamide chains within the array. Note that the actual crosslinks connecting adjacent polyamide chains are carbon–carbon double bonds. The resulting structure consists of crosslinked sheets of hydrogen-bonded chains.

Polydiacetylene chains are formed parallel to the stacking axis of the chains according to the schematic in Figure 1. Depending on the alignment of the diacetylene units within the ordered domains, the polydiacetylene chain could terminate in short sequences or in one long sequence spanning the entire ordered domain. Since the crosslinking reaction is actually a polymerization of diacetylene units, it is also referred to as a "cross-polymerization."

A whole host of diacetylene-containing polymers have been produced by condensation of a diacetylene-containing monomer with an appropriate comonomer. Diacetylene-containing polyurethane copolymers have been synthesized so that the diacetylene units reside only within the hard segments.[4] This ensures that diacetylene cross-polymerization occurs only within the hard domains formed preferentially by the hard segments of the polymer molecules. In many diacetylene-containing polymers, a diacetylene unit exists in every repeat unit along the chain and therefore ends up in amorphous as well as in crystalline regions. Even so, numerous studies, including the present one, have shown that crosslinking is primarily restricted to crystalline regions by controlled annealing or controlled exposure to ionizing radiation.[5] Above some threshold annealing temperature or radiation dose, the diacetylenes within the amorphous regions, which are simply unsaturated functional groups, can be made to react. This reaction, however, is most probably not the clean diacetylene to polydiacetylene conversion depicted in Figure 1.

Thus, under controlled conditions, crystalline regions of some semicrystalline polymers can be crosslinked without destruction of the crystallites. One of the materials in which this has been demonstrated is a flexible polyamide called PADA 6,22.[6] It is a polyamide–diacetylene synthesized from a 6-carbon diamine and a diacetylene-containing 22-carbon diacid. Thus, the diacetylene units exist within both the crystalline and noncrystalline domains of the polymer. The pre- and postcrosslinked primary structures of this poly-

mer are shown in Figure 1. Fibers of these polymers have been spun, and stress–strain curves have been reported as a function of radiation dosage.[7] The melt transition, 160°C for the nonirradiated polymer,[6] disappears upon irradiation. The present study examined the thermorheological consequences of crystalline-phase crosslinking in these polyamide fibers. Interference microscopy was employed as an indirect probe of polydiacetylene crosslink formation in oriented polymer fibers. Torsional moduli and dynamic mechanical properties of the initial and cross-polymerized fibers were compared to determine the influence of cross-polymerization on these properties. The mechanical stability of cross-polymerized PADA 6,22 at elevated temperatures was explored using thermal stress (TSA) and thermal deformation (TDA) analyses.

EXPERIMENTAL

The fibers were formed by wet-spinning from hexafluoroisopropanol solutions into a methanol coagulating bath. An average diameter of 25 μm was measured for the drawn filaments using the laser diffraction technique[8] (He—Ne, λ = 632.8 nm). Measurements were taken at four points along the length of every 1-in. sample and the mean was calculated. Crosslinking was achieved by exposure to controlled dosages of high-energy electrons from a Van de Graff accelerator operated at 2.6 MeV. Irradiations were done in air; care was taken to minimize sample heating.

Fiber X-ray diffraction patterns were obtained with a pinhole-collimated flat-film camera setup on an Enraf Nonius Delft Diffractus 583. Fiber bundles were exposed to the beam for 24 h in a vacuum-evacuated chamber before and after a 40 Mrad dose of electrons. The sample-to-film distance was 49 mm for a maximum scattering angle of about 38° 2θ. Wide-angle X-ray diffractograms were recorded on a Rigaku system with a rotating anode generator operating at 50 kV and 60 mA to produce slit-collimated CuKα radiation which was filtered through a thin Ni film. Samples were measured in reflection mode at step intervals of 0.05° for counting times of 2 s each.

The refractive indices with the plane of polarization parallel and perpendicular to the fiber axis were measured using an Aus Jena transmitted light interference microscope (λ = 550 nm). The fringe displacements in the parallel and perpendicular polarizations were measured at two points along the fiber length. Birefringence (Δn) and isotropic refractive index (n_{iso}) were calculated using[9]

$$\Delta n = n_{\parallel} - n_{\perp} \tag{1}$$

$$n_{iso} = \frac{(n_{\parallel} + 2n_{\perp})}{3} \tag{2}$$

where $n_{\parallel}$ and $n_{\perp}$ are the refractive indices in the parallel and perpendicular directions, respectively.

Dynamic mechanical properties were evaluated in the tensile deformation mode with a Seiko DMS 210. Sample lengths of 6.35 mm were subjected to a strain amplitude of 40 μm and test frequency of 3 Hz. The tests were conducted over a temperature range of −100 to 175°C, which allowed effective monitoring of the primary α transition and one of the secondary transitions.[10] Shear moduli were measured using a torsion pendulum apparatus. For circular fibers, the shear modulus is given by[11]

$$G = \frac{8\pi IL}{T_0^2 r^4} \tag{3}$$

where G is the fiber torsional modulus, I is the moment of inertia of rotating mass, L is the fiber length, T_0 is the time period of free, undamped, angular oscillations, and r is the fiber radius. The measured time period was corrected for damping with[12]

$$T_0 = \frac{T}{\left[1 + \left\{\frac{\Delta}{2\pi}\right\}^2\right]} \tag{4}$$

where Δ is the logarithmic decrement defined as $\ln(A_0/A)$; A_0 and A are amplitudes in successive oscillations.

Thermal stress (TSA) and thermal deformation (TDA) analyses[13] were conducted on a Seiko TMA/SS 2200. For the purpose of TSA, the extension was adjusted to achieve an initial force of 1 MPa. In the TDA scans, a constant force of 10 MPa was used. In both cases, fibers with initial sample lengths of 6.35 mm were heated at 5°C/min.

RESULTS AND DISCUSSION

Using laser diffractometry, it was found that the radius along a single-filament specimen varied

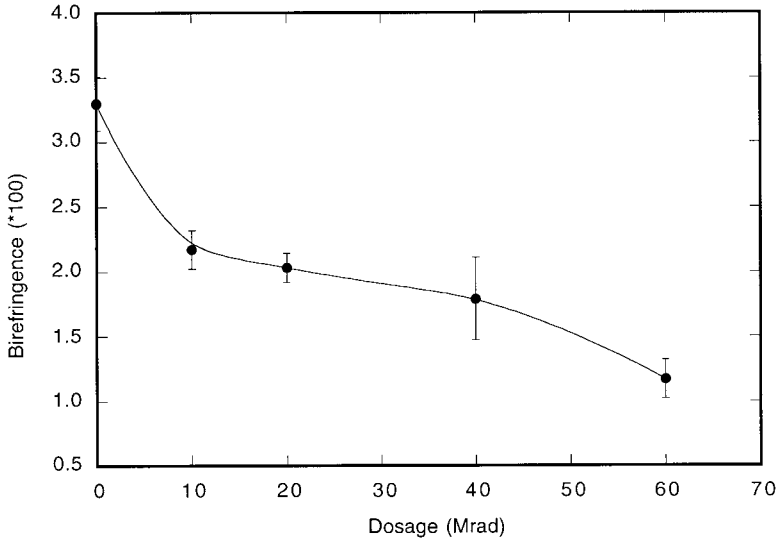

Figure 2 Birefringence (Δn) of PADA 6,22 fibers as a function of radiation dosage.

significantly ($\pm 15\%$). Possibly a result of uneven drawing, this irregularity in fiber radius strongly influences measurements of torsional moduli and birefringence. Thus, each birefringence measurement is based on the fiber radius measured at the corresponding position on that filament, and torsional moduli are reported as normalized data so that trends as a function of radiation dosage may be examined.

Figure 2 shows that the birefringence decreases as a function of radiation dosage, indicating that the fiber is becoming more optically isotropic upon irradiation. The birefringence values were calculated from the refractive indices, $n_{\parallel}$ and $n_{\perp}$, shown in Figure 3 along with n_{iso} calculated from the same values. While the $n_{\parallel}$ decreases, the $n_{\perp}$ and n_{iso} increase with radiation dosage.

An increase in refractive index in a particular direction can be caused by the reorientation of existing bonds or by the formation of new bonds, especially those that are highly polarizable. Figure 4 shows the X-ray scattering for a bundle of fibers before and after 40 Mrad of electron-beam radiation. The narrow azimuthal spread of the reflections shows that the crystals are aligned, and the alignment is not significantly affected by the irradiation. Previous solid-state NMR measurements have proven that the polydiacetylene crosslinks are formed from the diacetylene units.[7] Thus, the refractive index changes observed in Figure 3 are most likely related to the diacetylene cross-polymerization in an oriented system as depicted in Figure 1. The schematic shows the diacetylene units in an oriented fiber are largely parallel to the fiber axis before cross-polymerization. Upon radiation exposure, *diacetylene* units are converted into *polydiacetylene* crosslinks which are largely perpendicular to the fiber axis. Thus, the formation of the polydiacetylene crosslinks is reflected macroscopically as an increase in $n_{\perp}$ and an accompanying decrease in $n_{\parallel}$ as the corresponding diacetylene units are converted.

Figure 3 also shows that an increase in the average n_{iso} is observed for cross-polymerized PADA 6,22. Molecular bonding modifications of materials may be manifested as changes in isotropic refractive indices (n_{iso}) since these are related to individual bond polarizabilities. Whether the observed increase is appropriate can be revealed by a calculation of the difference in polarizabilities of a PADA 6,22 repeat unit before and after cross-polymerization. By summing the constituent isotropic bond polarizabilities,[14] the isotropic polarizability of a repeat unit can be estimated. The isotropic refractive index is then computed using the Lorentz–Lorenz relationship[15]:

$$\frac{n_{iso}^2 - 1}{n_{iso}^2 + 1} = \frac{4\pi}{3}\frac{P}{V} \tag{5}$$

where P is the isotropic polarizability and V is the volume.

Using values obtained from wide-angle X-ray diffractograms[16] to calculate the repeat-unit volume, the isotropic refractive index of the crystalline phase before cross-polymerization was calculated to be 1.530. Assuming a constant repeat-

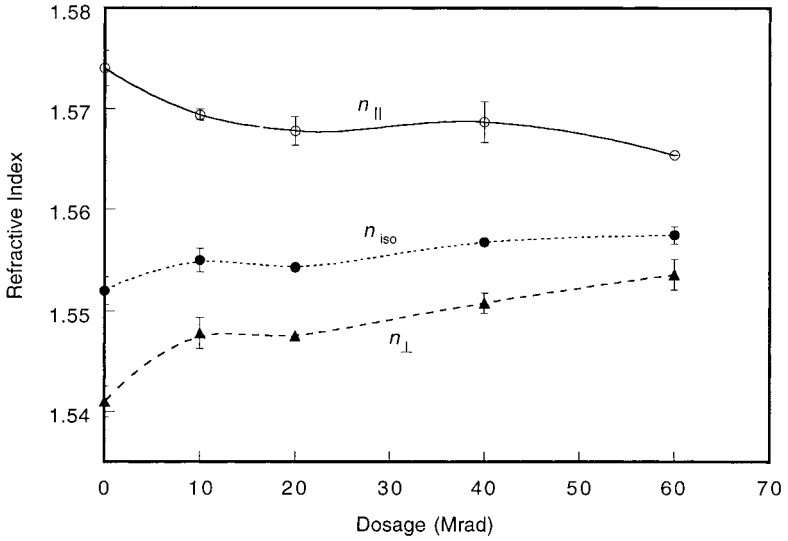

Figure 3 Refractive indices of PADA 6,22 fibers as a function of radiation dosage. The refractive indices parallel ($n_{\parallel}$) and perpendicular ($n_{\perp}$) to the fiber axis were used to compute the isotropic refractive index (n_{iso}).

unit volume, the isotropic refractive index after cross-polymerization was estimated to be 1.533, an increase of 0.003 units. A constant volume was assumed since no data are available on the three-dimensional changes of a repeat unit upon cross-polymerization. The calculated increase is simply due to the net conversion of one carbon–carbon triple bond to one carbon–carbon double bond and one carbon–carbon single bond. The diacetylene unit, which contains 2 C≡C's and 2 C—C's, is converted to a polydiacetylene crosslink, which contains 1 C≡C, 1 C=C, and 3 C—C's:

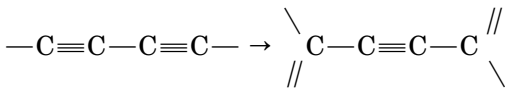

Any decrease in repeat-unit volume would result

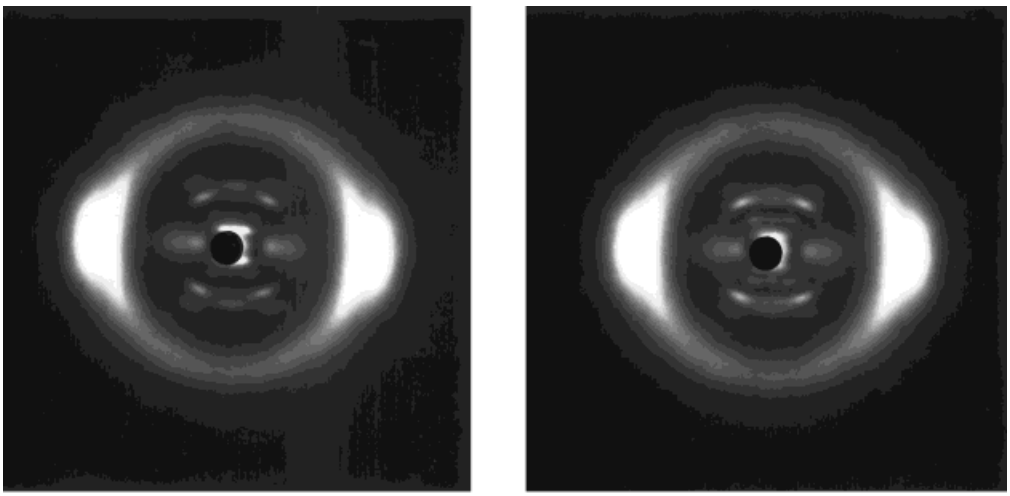

Figure 4 Wide-angle X-ray fiber patterns of PADA 6,22 fibers before and after 40 Mrad of electron-beam irradiation. Maximum scattering angle is about 38° 2θ.

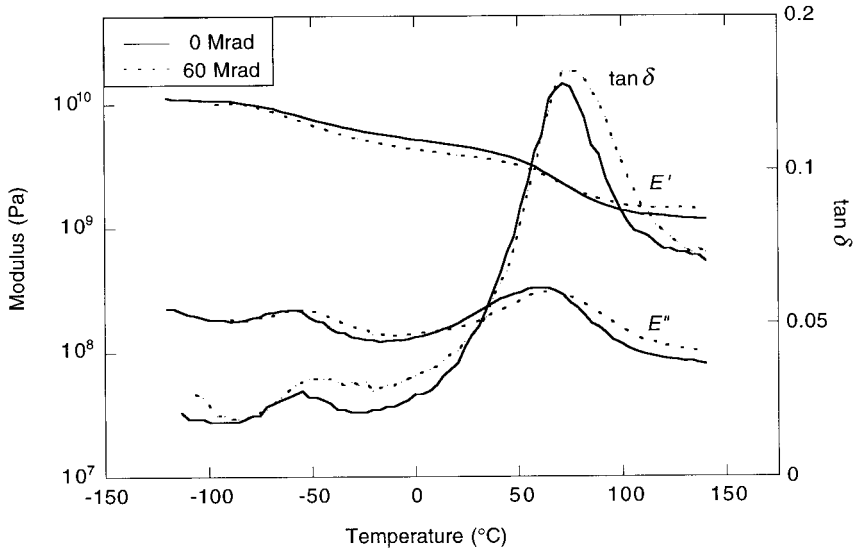

Figure 5 Dynamic mechanical thermal analysis of PADA 6,22 fibers before and after exposure to 60 Mrad of electron-beam radiation. E' is the storage modulus, E'' is the loss modulus, and tan δ is the loss factor = E''/E'. Test frequency was 3 Hz.

in even further increases computed for n_{iso}. The experimentally observed n_{iso} increases from 1.552 to 1.557, an increase of 0.005 units. Thus, the trend is the same for the values computed and those determined experimentally.

Figure 5 shows the DMS scans for PADA 6,22 at 0 and 60 Mrad of electron-beam irradiation. The T_g of the unirradiated PADA 6,22 can be seen as the maximum of the loss tangent curve at about 70°C. A second transition occurs at approximately −60°C and has been attributed to the onset of localized motions in the vicinity of the amide groups.[10] These two transition temperatures are listed in Table I as a function of radiation dose. On irradiation of the polymer, there is no statistically significant change in the transition temperatures. Even if some degree of amorphous-phase crosslinking is occurring at the higher radiation dosages, it is not conclusively revealed in the data of Figure 5. Crystalline-phase crosslinking obviously has no significant effect on the dynamic mechanical properties.

Table I Dynamic Mechanical Transition Temperatures of PADA 6,22 (Test Frequency = 3 Hz)

Dosage (Mrad)	β Transition Temperature tan δ (°C)	α Transition Temperature tan δ (°C)
0	−58.5 ± 3.2	72.0 ± 5.3
10	−56.4 ± 5.8	71.8 ± 2.9
20	−60.4 ± 6.8	73.0 ± 7.3
40	−62.9 ± 6.3	76.1 ± 1.9
60	−59.2 ± 5.9	76.0 ± 2.2

The torsional modulus of PADA 6,22 was monitored as a function of temperature and radiation dosage. The data are shown in Figure 6 as a function of radiation dosage after normalization to the values at 30°C for each respective radiation dose. For the temperature range studied, there is generally a decrease in torsional modulus with increasing temperature. Crystalline-phase crosslinking has no effect on this trend.

Thermal stress analysis (TSA) shows the development and decay of shrinkage stresses in materials held at constant length as a function of temperature.[17] In oriented semicrystalline polymers, a buildup of shrinkage force begins near T_g. This force, due to motions of oriented chain segments in the noncrystalline regions, increases with temperature as the numbers of mobile chain segments increases. This continues until the shrinkage forces in individual segments begin to exceed the force necessary to cause sliding of connected segments from the crystals, thus resulting in a decay of the cumulative shrinkage force. As the melting temperature is approached, almost all the chains anchored in the crystalline domains are released, thus contributing to a complete decay of shrinkage force. The temperature at which

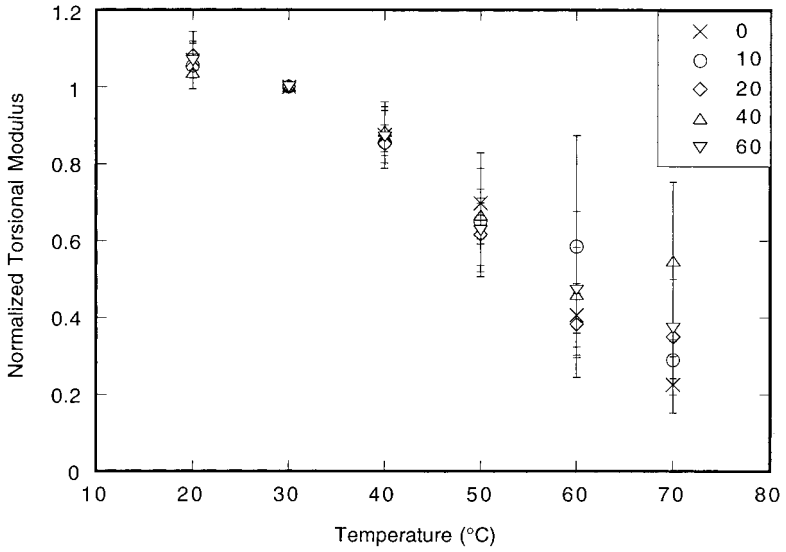

Figure 6 Normalized torsional modulus of PADA 6,22 fibers as a function of temperature. The torsional modulus at each temperature is divided by the torsional modulus at 30°C so that the radiation-induced changes in the curve shapes may be examined. Numbers indicate dosage in Mrad.

the shrinkage stress exhibited by the polymer becomes negligible is taken as the effective thermomechanical melting temperature.

The TSA scans for PADA 6,22 are shown in Figure 7 as a function of radiation dosage. All fibers show the initial stress buildup with increasing temperature. The nonirradiated fiber exhibits a maximum shrinkage force of about 0.1 cN/dtex at 55°C, followed by a decay up to an effective thermomechanical melting temperature of 200°C. Upon irradiation, the maximum shrinkage stress decreases and occurs at higher temperatures. The fibers exposed to 10 and 20 Mrad of radiation generally exhibit stress decay following the peak shrinkage stress similar to the nonirradiated fiber. The fibers exposed to 40 and 60 Mrad of radiation do not exhibit the same relatively rapid stress decay, but are able to maintain the maximum shrinkage stress of about 0.07 cN/dtex (8 MPa) to temperatures as high as 175°C. Thus, at tem-

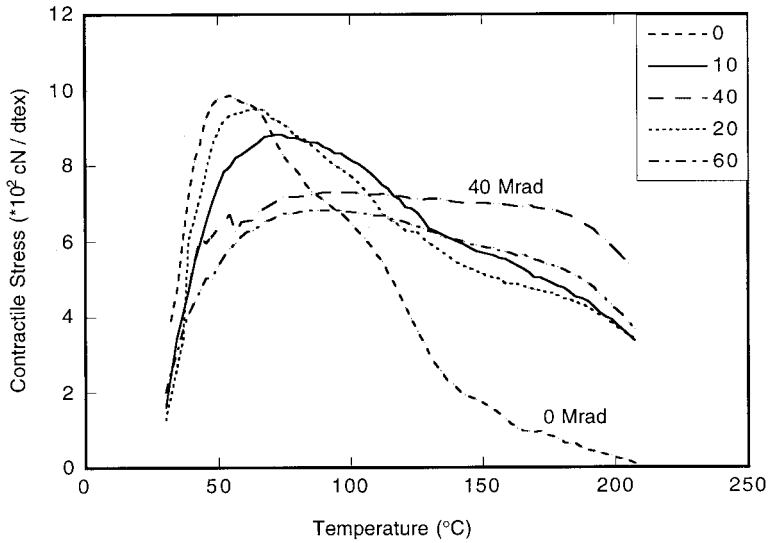

Figure 7 Thermal stress analysis of PADA 6,22 fibers as a function of radiation dosage. Numbers indicate dosage in Mrad.

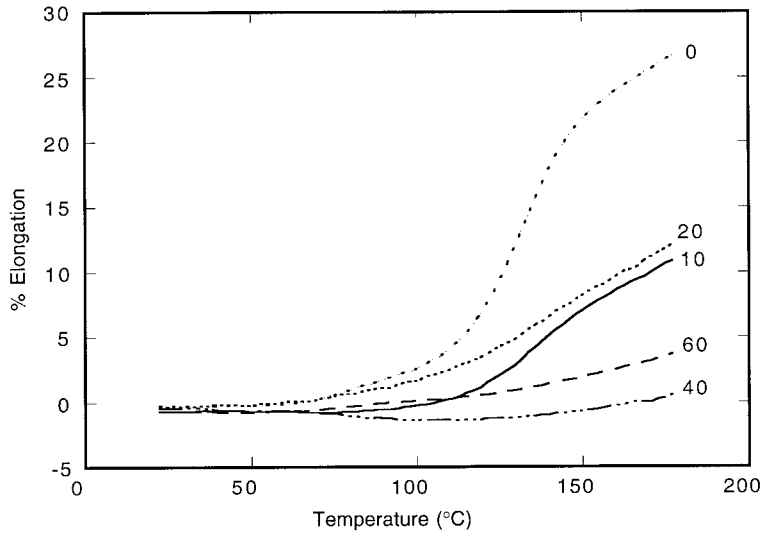

Figure 8 Thermal deformation analysis of PADA 6,22 fibers as a function of radiation dosage. Numbers indicate dosage in Mrad.

peratures close to the effective thermomechanical melt temperature of the nonirradiated fiber, the crystalline-phase-crosslinked fibers are still able to retain shrinkage stresses.

Since the maximum shrinkage stress decreases as a function of radiation dose, the irradiation must result in some type of structural change. A possible explanation is orientational relaxation within the fiber due to the heating encountered during irradiation. If this occurs, the potential for chain coiling is reduced, thereby leading to reduced maximum shrinkage stresses. The X-ray photographs of Figure 4 show no orientational relaxation of crystalline regions, but cannot reveal that which may occur in amorphous regions. According to the TSA scan of the nonirradiated fiber in Figure 7, the temperature only needs to reach about 55°C for relaxation to occur.

The TSA results are supported by those from thermal deformation analysis (TDA), which measures length changes at a constant applied force as a function of temperature.[18] In the TDA scans of Figure 8, the nonirradiated PADA 6,22 fiber exhibits a sharp increase in extension at a temperature of about 120°C, well above the glass transition. At the same temperature, the fibers exposed to 10 and 20 Mrad of radiation also reveal a slope change in the extension versus temperature curves, but the increase is not nearly as sharp. The fibers exposed to 40 and 60 Mrad of radiation exhibit no distinct transition in the extension vs. temperature curves at 120°C, but only gradual increases in extension up to 175°C. The nonirradiated fiber exhibits a second inflection point at 150°C, after which the extension increases at a much lower rate than in the region between 120 and 150°C. This is most probably caused by thermally induced crosslinking that occurs during the scan. Evidence for this is the simple fact that strain values can be measured for the nonirradiated fiber at temperatures greater than 160°C, the melt temperature of the noncrosslinked polymer.[6]

The retention of shrinkage force and lower extensions at close to melting temperatures is due to the resistance of the polymer chains to pull out of the crystalline domains, which are now crosslinked. Thus, the structural integrity of the material has been enhanced. This result of crystalline-phase crosslinking could have useful consequences. For example, many polymeric materials creep, resulting in reduced performance as a function of time.[19] Crosslinking the crystalline domains could be a useful method of inhibiting gradual slippage of chains from the crystalline domains over long periods of time. Also possible is the improvement of structural integrity in materials without adversely affecting diffusional characteristics of small-molecule penetrants.

Examination of all data as a function of radiation dosage suggests a change in material response to the radiation at dosages greater than 20 Mrad. The birefringence and refractive index data of Figures 2 and 3 exhibit a small plateau region for low radiation dosages that no longer exists for dosages greater than 20 Mrad. The TSA and TDA scans suggest the fibers respond differ-

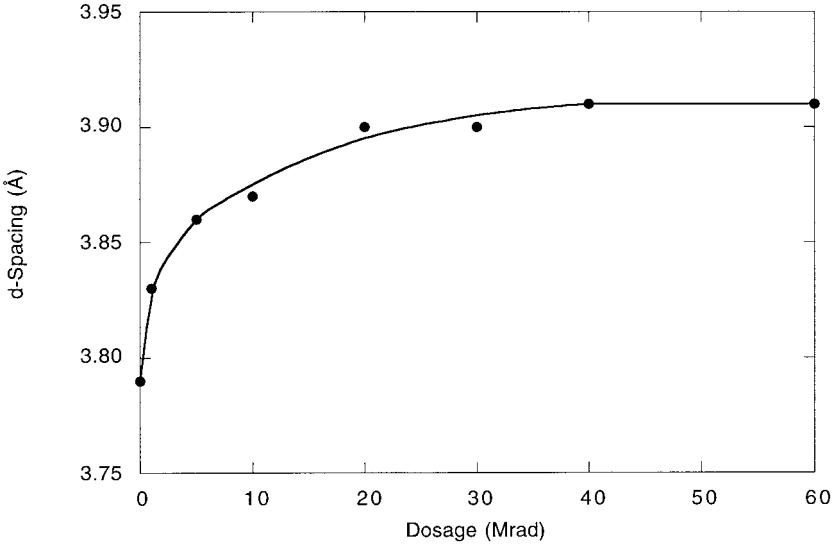

Figure 9 Crystalline d_{010} interplanar spacing (uncorrected for size and inhomogeneous strain effects) versus radiation dosage from wide-angle X-ray diffractograms of PADA 6,22.

ently to radiation doses of 40 Mrad and greater, as compared to the lower radiation dosages. Figure 9 shows the apparent* interplanar d_{010} spacing from wide-angle X-ray diffractograms as a function of radiation dosage. Described in detail elsewhere,[16] this d-spacing represents the distance between the hydrogen-bonded sheets of polyamide chains of PADA 6,22. Upon cross-polymerization, an expansion along this direction within the crystal is necessary for the diacetylenes to convert to polydiacetylene crosslinks. The data of Figure 9 indicate that the d-spacing levels off beyond 20 Mrad. Taken together, the data suggest the threshold dosage for restriction of crosslinks to crystalline regions in these fibers is between 20 and 40 Mrad. Up to 20 Mrad, the crosslinks are created in the crystalline phase via a diacetylene-to-polydiacetylene conversion. For dosages of 40 Mrad and greater, the unsaturated diacetylene functionality may be reacting via other routes as well.

CONCLUSIONS

Diacetylene-containing polyamide fibers may be crosslinked in the crystalline phase by controlled exposure to electron-beam radiation. In an oriented fiber, the polydiacetylene crosslinks are formed perpendicular to the fiber axis. For radiation dosages up to 60 Mrad, the dynamic mechanical properties and torsional moduli are not significantly affected. Crystalline-phase crosslinking results in fibers that support shrinkage stresses and exhibit substantially lower creep at close to melting temperatures of the uncrosslinked material. This mechanism in materials may be useful in applications which require higher-temperature performance without destroying amorphous-phase chain mobility and accessibility.

The Polymer Program Associates of Georgia Tech are gratefully acknowledged for partial stipend support. The authors thank Dr. Vinay Mehta, Ronny Grindle, and Sam Sheffield for their contributions while at Georgia Tech. Ken Wright of the MIT High Voltage Research Laboratory performed the electron-beam irradiations. The fibers were spun at the DuPont Experimental Station due to the efforts of Dr. Michael Rubner and Dr. Len Buckley, with funding provided by ONR.

REFERENCES

1. (a) N. Sasaki, T. Yokoyama, and T. J. Tanaka, *J. Polym. Sci. Part A,* **11,** 1765 (1973); (b) W. Dzierza, *J. App. Polym. Sci.,* **22,** 1331 (1978); (c) S. L. Cooper and A. V. Tobolsky, *J. App. Polym. Sci.,* **10,** 1837 (1966).
2. G. Wegner, *Makromol. Chem.,* **154,** 35 (1972).
3. (a) V. Enkelmann, *Adv. Polym. Sci.,* **63,** 91 (1984);

* Uncorrected for size and inhomogeneous strain effects.

(b) H. Gross, H. Sixl, C. Kröhnke, and V. Enkelmann, *Chem. Phys.,* **45,** 15 (1980).
4. (a) M. F. Rubner, *Macromolecules,* **19,** 2114 (1986); (b) R. A. Nallicheri and M. F. Rubner, *Macromolecules,* **23,** 1005, 1017 (1990).
5. H. W. Beckham and H. W. Spiess, *Macromol. Chem. Phys.,* **195,** 1471 (1994).
6. H. W. Beckham and M. F. Rubner, *Macromolecules,* **22,** 2130 (1989).
7. H. W. Beckham and M. F. Rubner, *Polymer,* **32,** 1821 (1991).
8. A. J. Perry, B. Ineichen, and B. Eliasson, *J. Mater. Sci. Lett.,* **9,** 1376 (1974).
9. R. Srinivasan, P. Desai, A. Abhiraman, and R. Knorr, *J. App. Polym. Sci.,* **53,** 1731 (1994).
10. W. P. Leung, K. H. Ho, and C. L. Choy, *J. Polym. Sci.,* **22,** 1173 (1984).
11. V. Mehta and S. Kumar, *J. Mater. Sci.,* **29,** 3658 (1994).
12. R. J. Young, *Introduction to Polymers,* Chapman and Hall, New York, 1983, Chap. 5.
13. M. Jaffe, *Thermal Characterization of Polymeric Materials,* E. A. Turi, Ed., Academic Press, Orlando, FL, 1981, p. 731.
14. (a) K. G. Denbigh, *Trans. Faraday Soc.,* **36,** 936 (1940); (b) C. G. Le Fevre and R. J. W. Le Fevre, *Rev. Pure App. Chem.,* **20,** 57 (1970).
15. E. Riande and E. Saiz, *Dipole Moments and Birefringence of Polymers,* Prentice Hall, New York, 1989, p. 201.
16. H. W. Beckham and M. F. Rubner, *Macromolecules,* **26,** 5192 (1993).
17. (a) D. R. Buchanan and G. L. Hardegree, *Tex. Res. J.,* **47,** 732 (1977); (b) K. Yoon, P. Desai, and A. S. Abhiraman, *J. Polym. Sci. Part B.,* **24,** 1665 (1986).
18. P. Desai and A. S. Abhiraman, *J. Polym. Sci. Part B.,* **26,** 1657 (1988).
19. (a) H. Leaderman, *Elastic and Creep Properties of Filamentous Materials and Other High Polymers,* The Textile Foundation, Washington, DC, 1943, Chap. 3; (b) G. R. Moore and D. E. Kline, *Properties and Processing of Polymers for Engineers,* Prentice-Hall, Englewood Cliffs, NJ, 1984, p. 112.